Proceedings of ASME Turbo Expo 2011
GT2011
June 6-10, 2011, Vancouver, British Columbia, Canada

GT2011-45223

CONTROLLED FAN BLADE TIP/SHROUD RUBS AT ENGINE CONDITIONS

Corso Padova
Gas Turbine Laboratory
The Ohio State University

Michael Dunn
Gas Turbine Laboratory
The Ohio State University

Jeffrey Barton
Gas Turbine Laboratory
The Ohio State University

Kevin Turner and Tod Steen
GE Aviation
Cincinnati, OH

ABSTRACT

The purpose of this paper is to describe the new facility design and operation improvements, and to demonstrate utility by providing typical results obtained as part of a typical measurement program. Since 2002 a number of experiments have been conducted to generate a broad database for tip rubs using two unique experimental facilities at the Gas Turbine Laboratory of The Ohio State University. Development of an in-ground spin-pit facility specifically designed to investigate rub-in-systems for jet engine components using real hardware rotating at representative engine speeds was reported several years ago. While the original smaller facility is still in use, more recently a much larger in-ground spin-pit facility for which the basic design and operation of the blade tip/shroud incursion technique is very different from the original facility design has been commissioned, and the results of a measurement program completed using a full-scale titanium-alloy fan blade rubbing an abradable casing are presented.

The Large Spin-Pit Facility [LSPF] is designed to allow rotating engine hardware from low RPM [typically a few thousands] to 18,000 rpm, using two interchangeable spindle arrangements mounted above ground onto an in-ground containment tank. The LSPF is also designed to allow the progressive insertion of a casing segment into the path of a single-bladed or multiple-bladed disk. Segments extending 90 or 120 degrees are in use for different applications. For the configuration discussed in this paper, a 90-degree segment of a representative fan casing is forced to rub the tip of a titanium-alloy fan blade at a rotational speed in the vicinity of 6000 rpm.

1. INTRODUCTION

Since 2002 experiments on tip rubs of bladed compressor disks rotating at representative engine speeds have been conducted in a special purpose in-ground Spin-Pit Facility (SPF), which was developed at the Gas Turbine Laboratory of The Ohio State University (GTL). The initial development of the compressor facility capable of spinning bladed disks at rotational speeds up to 20,000 rpm and specifically designed to investigate aeromechanic phenomena for gas turbine engine hardware was first reported by Padova et al. [1]. The research interest envisioned from the inception of this facility design dictated the layout of its key components: (a) a high-stiffness spindle, (b) a fast-acting mechanism that allows insertion of the engine casing into the path of the bladed rotor, (c) a casing sector mounted on a rigid transfer bar that is backed by piezoelectric load cells. Results from the operation of the compressor facility were reported in successive papers [2,3]. A number of experiments were conducted to generate a broad database for tip rubs, the Rotor-Blade Rub Database (RBR database). As of 2010, there are nine completed groups of measurements in the database. Within these groups are a number of blade-tip geometries, blade materials and casing surface treatments that have been investigated.

In the development of the facility and experimental results noted above, considerable emphasis was placed on engine manufacturer input regarding the facets of the rub phenomena where results would yield the highest design-advance payoff. Characterizing blade impact dynamics for compressor stages of typical dimensions was high on this list. Hence the GTL Compressor SPF included a cylindrical underground containment tank of suitable size (1.52 m in diameter by 0.65 m high [5 by 2.1 ft]) and has 0.90 m (3 ft) diameter openings at the top and at the bottom. The fast-acting mechanism provides a given number of highly repeatable blade incursions to investigate specifically the blade impact dynamics using measurements from strain gauges carefully located on the blade to monitor predicted response modes and frequencies.

During the execution of the above investigations it became apparent that rub phenomena and loading conditions associated with blade tip/shroud interference for the entire compression

system and not only for the inner compressor stages were also of interest. Based on the successful approach already in operation, a new larger experimental facility was designed and constructed. It was quickly determined that a new in-ground SPF capable of testing full scale fan rotors in the 9 ton [20,000 lbf] thrust class, and scaled model of fan airfoils up to those used for the largest contemporary engines would yield the highest design-advance payoff for investigating future rub phenomena driven by advanced engine designs. The research interest envisioned from the inception of this facility design dictated a somewhat different layout of some of the key components. The emphasis was less on airfoil dynamics and more on rub forces on the casing, in particular those unsteady, destabilizing, geometry-induced forces which may contribute significantly to rotor whirl instabilities at the front end of the compression system. Field experience with such facets of the rub phenomena pointed to the potentially important role of incursion rate in determining the severity of rubs. Accordingly the Large Spin-Pit Facility (LSPF) was designed to incorporate a progressive incursion mechanism capable of providing ample control on rate of incursion and incursion depth between blades and shroud. The mechanism is described fully in section 2.2 of the paper. In addition the spindle arrangement was selected to include a variable damping component [described in section 2.1] to provide flexibility in controlling its rotordynamic response under various expected loading conditions. The purpose of this paper is to describe the development of the new experimental capability and to present results that demonstrate the operability of the facility and the importance of these results to the engine designer. Results from a recently completed set of measurements obtained for a wide chord, forward swept titanium alloy fan blade rubbing into an epoxy-treated casing are presented.

Contemporary gas turbines rely on complex blade-casing rub-in-systems to improve the tip clearance behavior during operation from initial service to maximum lifetime [4-6]. Typically, a rub-in-system in the compression section of the engine may consist of a specific circumferential area of the case shaped to accept coatings of materials selected for in-service wear and, when required, fire shielding. A momentary eccentricity of a few 1/10 ths of one millimeter (0.1 mm = 0.004 in) between a blade and the engine case, which may occur because of an abrupt maneuver in flight or in a hard landing, may cause the tips of a few airfoils to incur the rub-in surface and even initiate a potentially destructive whirl instability [7,8].

Blade-to-case rubs can degrade the operation of an engine through the induction of high amplitude shaft vibration and severe blade/seal wear, and may lead to shutdown of the engine in the worst occurrence. Precisely for these reasons, engines are already routinely tested for containment and survival of blade out events. But to enable the formulation of a comprehensive design methodology for rub-in-systems, particularly one that can predict and take advantage of the potential offered by new and emerging rotor/blade concepts, advances in several underlying technologies are needed.

In advanced compressors, the complexity of the flow field that must be carefully considered to obtain the desired high level of performance has driven development and use of refined computational models. The necessity of complex modeling for the compressor flow field also encourages the deployment of computational models that address the structural dynamic aspects of the phenomena. Computational models to analyze the non-linear dynamic response of a rotating beam with periodic pulse loading at the free-end [9-11] and rub casing loads [12] are thus under development. They aim to predict the dynamics of vibro-impact systems with multiple degrees-of-freedom and are needed to enable the formulation of a comprehensive design methodology for rub-in-systems.

In combination with continuing progress in other more mature allied technologies such as rotor dynamics under severe disturbances [13-15], forced vibrations of bladed disks [16,17], and characteristics of abradable materials [18,19], the improved understanding of the phenomena that affect blade-casing interactions is expected to result in savings in gas turbine maintenance costs applicable not only in propulsion engines but for stationary advanced power systems as well.

2. EXPERIMENTAL ARRANGEMENT

The arrangement of the Large Spin-Pit Facility (LSPF), which was specifically designed to investigate rub phenomena of full scale and scaled models of contemporary fan rotors at representative engine speed, is described in this section. The LSPF is capable of accommodating configurations with rotor diameters of up to 2.2 m (7.2 ft). The underground containment tank that houses both the rotating component and a high-stiffness spindle is cylindrical (2.4 m in diameter by 0.7 m high [7.9 by 2.3 ft]), and has 1.6 m (5.2 ft) diameter opening at the top and 90 degree sector access port at the bottom. Figure 1 is a photograph of the facility showing the large containment tank being lowered into the concrete reinforced trench during the early construction phase of the facility in part (a) and the facility during operation in part (b).

(a)

(b)

Fig. 1 View of the Large Spin Pit Facility: (a) the containment tank during construction and (b) the facility in operation.

Rub phenomena investigations dictate the use of a high-stiffness spindle capable of reacting to the transient forces generated during rotor contact to the casing. Based on the successful operation of the existing Compressor SPF, the LSPF design developed around the use of a vertical and high-stiffness spindle capable of operating at representative engine rotational speeds for a reasonable period of time. The system utilized here incorporates hybrid bearings and an oil mist lubrication system. This first major component of the LSPF will be described in more detail later in section 2.1 of the paper.

As noted in the Introduction a second major subsystem required to investigate blade-to-case rubs is an incursion mechanism that allows controlled insertion of the engine casing into the path of the bladed rotor. The LSPF was designed with a progressive incursion mechanism capable of providing ample control on rate of incursion and depth of incursion between blades and shroud. The research interest envisioned from the inception of this facility put emphasis more on rub forces on the casing than on airfoil dynamics.

In addition to the two major subsystems noted above, a few other unique facility design features are key in making the large facility a versatile tool for performing research on many areas of aeromechanics, including rubs, blade excitation, and blade dampers. A modern high-efficiency air turbine is used to spin-up rotors with large moment of inertia in a few minutes. Full vacuum [less than 2 torr] is maintained in the containment tank during operation to eliminate high air friction losses and to reduce the heating that may result from pumping even low-pressure air. A high capacity oil mist system is required to operate the hybrid ceramic bearings at high rotational speed [18000 rpm], and a custom contact carbon seal manufactured by Stein Seal Company is used to isolate the bearing chamber from the rotor chamber. The seal component is described in more detail later in section 2.1. To complete the design of the facility, a high-speed slip ring and hollow drive shaft is used to route strain gauge signals from an instrumented airfoil to the laboratory data collection instrumentation.

2.1 Drive System

The vertical spindle of the LSPF shown in Figure 2 is capable of operating at 7,000 rpm. It consists of a hollow shaft having 95.3 mm (3.75 in) outer diameter supported on large [170 mm, 6.7 in], ceramic hybrid, angular contact ball bearings. The shaft is driven from the top by a reversible air motor. The single stage engine rotor is bolted to a flange located approximately in the middle of the spindle assembly and is surrounded by the containment test chamber. Below the flange the shaft continues toward the bottom of the containment tank where it is constrained by a grease-lubricated third bearing unit. The bottom bearing is housed into an isolator assembly that consists of an inner bearing housing, axially preloaded, an outer housing and a radially compliant elastomer connecting the two parts. The isolator can be fitted with different membrane materials, thicknesses and clamping schemes. This allows a range of stiffness and damping values to be selected for control of the spindle rotordynamic characteristics.

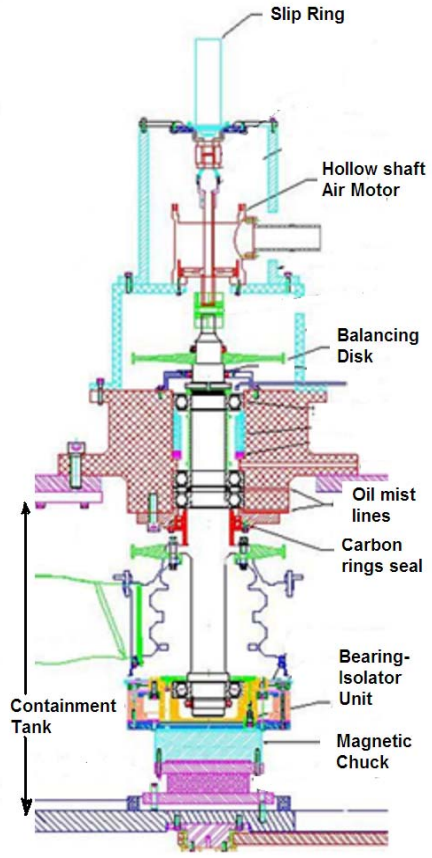

Fig. 2 Section of Spindle rated for 7000 rpm

The high-performance shaft seal noted above (Stein Seal) isolates the bearing cavity from the rotor cavity. The bearing housing is maintained above ambient pressure as a high capacity oil mist system lubricates the raceways and rolling elements. A buffer air supply is used to pressurize the space between the carbon rings. The seal design provides gas leakage of 19.5 liter/min (0.69 scfm) for the vacuum side, and 6 liter/min (0.21 scfm) for the bearing cavity side. The seal generates 0.27 kW (15.5 BTU/min) of frictional losses which is absorbed by the shaft and convected by the buffer/mist air flows.

Interchangeable key components are an important part of the LSPF versatility. The low-speed drive system described above is presently one of two systems available for use in the facility. A second interchangeable vertical spindle capable of operating at 18,000 rpm is available and follows the same general arrangement shown in Figure 2. The 66.8 mm (2.63 in) outer diameter hollow shaft is supported on small [100 mm, 3.9 in] high-speed, ceramic hybrid, angular contact ball bearings. Again, the shaft is driven from the top by a reversible air motor and the engine rotor is mounted beneath the spindle assembly and is surrounded by the containment test chamber.

Not shown in Figure 2, but integral to the drive system unit is an emergency brake capable of rapidly slowing and stopping the rotation of the rotor in case an anomaly occurs during the facility operation. The brake unit consists of a caliper-type automobile disk brake adapted to the drive system. To stop the wheel, friction pads are forced pneumatically against both sides of the disk.

2.2 Incursion Mechanism System

The LSPF uses a progressive Incursion Mechanism System (IMS) which is very different from that developed previously for the CSPF. A progressive IMS functions to move the engine case segment into the blade at the desired time for a programmable incursion rate ($\dot{\varepsilon}$) and maximum incursion depth (ε). For a single-bladed rotor, the number of blade strikes is determined by both variables and by the cycle time of the IMS. After the specified number of strikes and the desired incursion depth are achieved, the mechanism retracts the casing out of the blade path ending one IMS cycle.

For the results presented in this paper, a 90-degree sector of a representative engine casing is forced to rub the tip of a single bladed fan disk for a limited number of times with predetermined blade incursion into the casing. The speed at the time of rub was on the order of 6,000 rpm. At this rotational speed, the instrumented airfoil returns to the same circumferential position in 10.8 ms, thus the contacts between blade and shroud experienced before the interference is removed is directly proportional to the incursion (and retraction) rate and the programmed depth of incursion. The casing sector is mounted on a load-measuring unit based on three piezoelectric load cells [described in detail later in section 2.3] and attached to a support sector that slides in the horizontal plane.

The incursion mechanism consists of two major subsystems (structural and actuation). The structural subsystem consists of a support sector and two slides that carry the casing segment along during its motion, a linear actuator that controls the motion, and high-stiffness components anchoring all elements of the system to the containment tank cover. The actuation subsystem consists of the two parallel linear slides, the electric actuator and its associated controls and moves the load measuring unit and casing toward the spinning blades for rub experiments. The actuation subsystem includes a machining-quality positioning readout based on a glass linear encoder for precise control accuracy.

The function of the structural subsystem is to carry the casing segment that is mounted to the load-measuring unit (LMU) through its travel cycle into and back out of the blade path. Figure 3 shows a schematic of the structural subsystem and identifies its main elements. Figure 4 shows a picture of the subsystem installed in the containment tank of the facility. The LMU is attached to a support bracket that translates radially in and out toward the spindle. The support bracket consists of a stiff gusseted weldment made of steel. The bracket is bolted and pinned to the saddles of two parallel DuraBond precision slides. The linear slides feature a unique low profile, square gib, Rulon coated construction to provide high precision and rigidity with superior vibration dampening characteristics. Typical tolerances per 30.5 cm (12 in) length are 25.4 μm (0.001 in) flatness value and 12.7 μm (0.0005 in) tracking parallelism of base and saddle. The slides are arranged in a ceiling mount to the top lid of the containment tank in a layout that allows easy removal and full access to the entire IMS structural subsystem for precision adjustments relative to the spindle-rotor assembly. The LMU support bracket is attached to the moving rod of an EC5 electric cylinder. Rigid steel mount beams complete the structural subsystem by securing all components to each other and to the tank lid.

The actuation subsystem consists of the electric cylinder and its associated controls. The EC5 cylinder series offers heavy thrust loads [up to 25kN (5620 lbf)] and a range of travels. They employ precision rolled ballscrews, yielding quiet operation, low backlash and high accuracy [position repeatability -/+ 12.7 μm (0.0005 in)]. The EC5 model selected for the facility has 10 mm (0.4 in) ballscrews, 150 mm (5.9 in) travel, and is operated by a BK42 brushless servo motor. A B8962 two-axis digital servo drive and an Acu-Rite linear encoder and machining readout complete the subsystem. The servo drive is capable of controlling position, velocity, and force/torque simultaneously. It has a system resolution of 8000 counts and 8 digital programmable inputs. It offers both a programming and operator interface with a detachable front panel. The Acu-Rite position readout unit uses a SENC 150 precision glass linear encoder and a 200S display. The SENC 150 has a 20 μm (0.00079 in) grating pitch, a +/- 10 μm (0.00039 in) accuracy in a 1 m (3.28 ft) length, and a maximum slew speed of 102 cm/s (40 in/s). The 200S display is a milling

and grinding quality unit with precise error compensation and ISO-9001 certification.

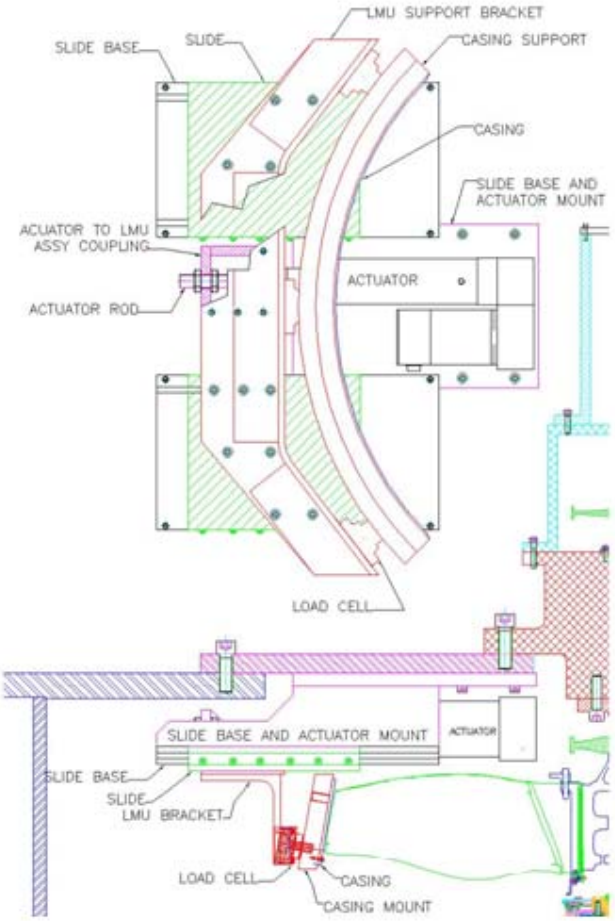

Fig. 3 Progressive Incursion Mechanism Schematic

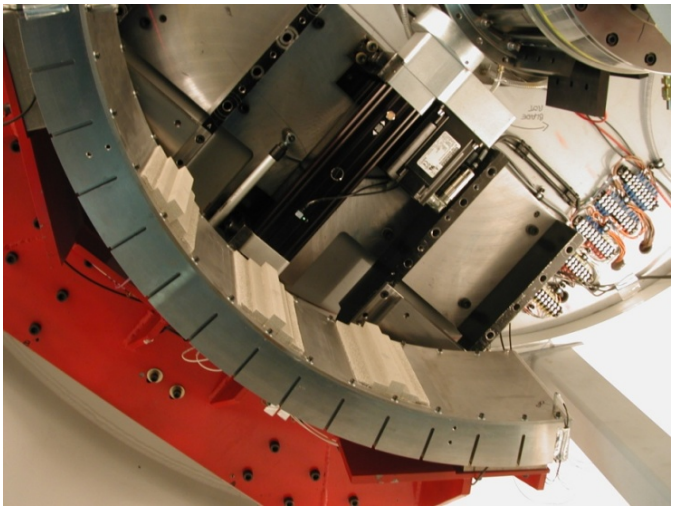

Fig. 4 Incursion Mechanism Photo

2.3 Load Measuring Unit

The segment of engine casing against which the blade rubs is carried by an instrumented support that includes three load cells. The design of the casing load measuring unit (LMU) was developed first for use on the Compressor SPF and was discussed in detail previously [1]. For the LSPF the LMU size had to be scaled up considerably, leading to concern about the total weight of the unit. Finite element analyses were performed to arrive at an improved design of the support bar which retains large stiffness with a reduced weight. This was obtained by using a ribbed cross-section as the basis of the support bar. Two units of different geometry are currently available for different setups in the LSPF. The LMU-G has a reference inner radius of 350 mm (13.8 in) and extends over an 88 degrees sector. The LMU-H has a reference inner radius of 221 mm (8.7 in) and extends over a 120 degrees sector. For the results presented in this paper, the LMU-G was installed and is discussed in what follows.

LMU-G uses three Kistler Mod. 9067B piezoelectric load cells so arranged to measure nine components of force. The two end cells are placed below the load line, which is located in the mid plane of the engine case, and the center cell is located above the load line. The arrangement is designed to minimize the moment loads on each cell and to obtain moment information around three mutually perpendicular axes from the entire unit. Five accelerometers are also mounted on the LMU shown in Figure 5. Three radial directions are measured at locations very close to each load cell. A tri-axial block mounted near the center load cell is equipped with the remaining two accelerometers that measure one axial and one circumferential direction in the middle of the LMU.

In contemporary engine fans the casing consists of a multi-component structure, which must satisfy stringent blade-out containment requirements. The inner layer of the casing structure for these experiments was a high-density Epoxy material that doubles as an abradable coating in the fan assembly. The Epoxy material was applied on the LMU thin metal casing following the same process used for production engines. As for the engine, the radius of the casing cylinder is greater than the radius of the circular path followed by the blade tips under normal operating conditions. A tight but finite clearance is maintained at the rub-in-system surface. This condition is applied to ensure that no impact of the blade will occur first at the edge of the LMU for all chosen values of eccentricity between casing and rotor in the experiments. In addition, the corners of the casing sector are beveled for added margin of safety.

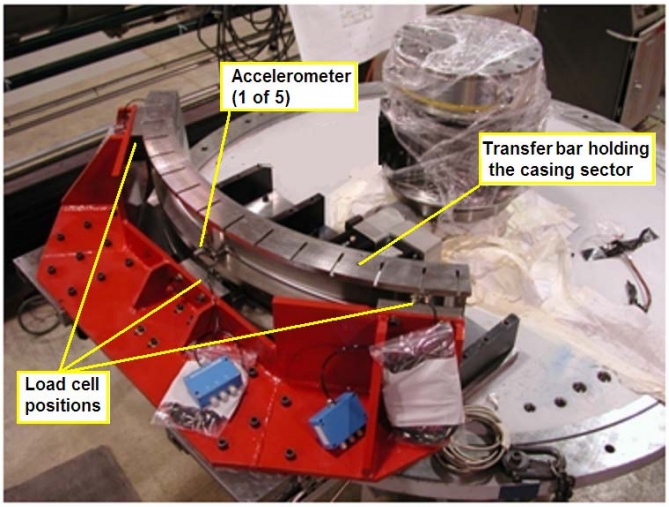

Fig. 5 Load Measuring Unit

3. OPERATION

During a typical experiment the rotor is spun-up to the target speed in about three minutes. During this time the inertial forces reacting to the centripetal acceleration increase and cause the rotor and blade to elastically deform to an instantaneous shape that is different from the static geometry: in particular, the airfoil "unwraps" under flexural, torsional and shear loads. As the rotor speed approaches the target value selected for a rub to occur, the angular acceleration is gradually decreased so that the airfoil impact with the shoe occurs effectively at a constant value of rpm. The rub sequence is initiated by activating the motion controller (described later in this section) to move the casing toward the spinning blade tip. This results in a constant speed movement [constant incursion rate $\dot{\varepsilon}$] of the casing toward the closest part of the spinning blade tip. At some point during the casing motion, the tip sweep line is crossed, and the initial rub of the blade onto the casing occurs. Figure 6 (a) shows a time history of the many rub events over a time period from 1.2 s to 2.9 s with the first rub occurring in the second revolution, which is displayed at time t = 1.287 seconds. The figure shows the markers for three sensors. All sensors respond to the specific experimental event with a momentary change in voltage which is displayed on the ordinate of the plot. The baseline values or magnitude of the recorded voltages are not significant as the sensors are designed only to mark the event in time. Two of the three sensors are optical, blade-passage indicators. They give the red and green lines in the plot as the blade begins and ends the sweeping motion over the casing. The third sensor [blue lines in the plot] indicates contact between the blade and the shoe. For the case shown in the figure the rub speed was set at 100% test-point rpm, one revolution lasts 10.8 ms, sweeping of the blade over the casing occurs in 2.7 ms. The time span of the figure shows about six revolutions. From left to right, revolution 1 generates no rub, revolution 2 generates a light rub, indicated by the electrical contact signal that appears between the markers, and revolution 3 like all the following ones generate more light rubs.

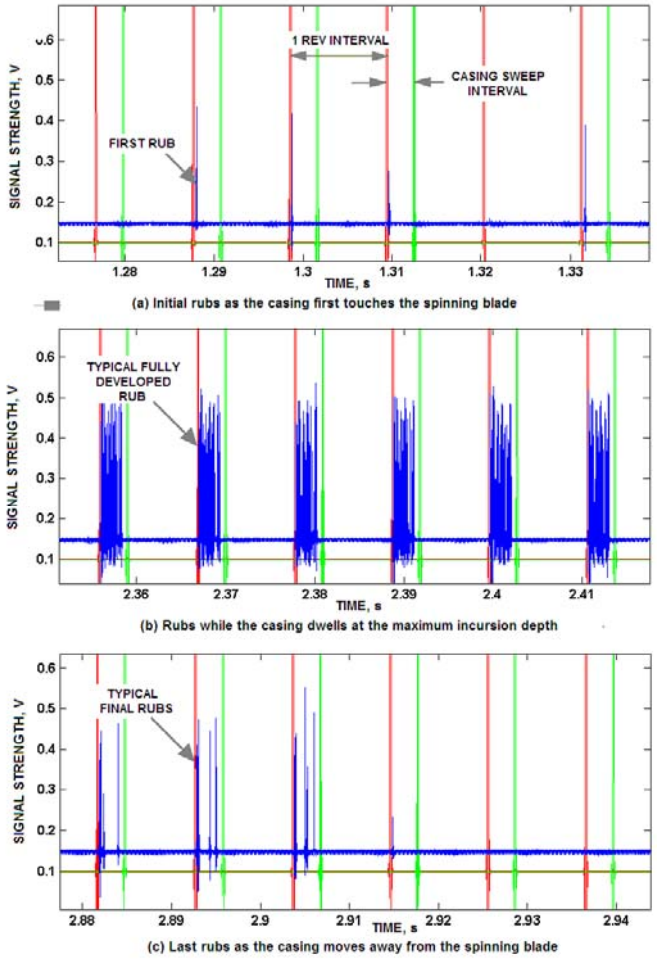

Fig. 6 Rubs during Casing Motion and Maximum Incursion Region

For the case shown in Figure 6, the incursion rate had been programmed to be 635 µm/s (0.025 in/s) to a maximum incursion depth of 635 µm (0.025 in). When the first contact between casing and blade occurs, the motion controller allows for a change to a different incursion rate if so desired. However, for the case shown the incursion rate remained constant at 635 µm/s (0.025 in/sec), and a second deeper rub was obtained as soon as the blade returned over the LMU sector. The greater the incursion depth, the more rubs occur before the casing locks into a casing dwell region [$\dot{\varepsilon} = 0$ and ε at maximum chosen value]. Figure 6(b) shows six rubs obtained in the dwell region. Depending on factors traceable to the blade geometry and dynamics, the most severe rubs will occur before or during the casing dwell time interval. Here the features of the contact signal in Fig. 6(b) indicate more severe rubs than those shown in Fig. 6(a).

After the programmed dwell time has expired the casing was retracted at constant speed. The blade is still vibrating and initially a number of contacts with the casing are still possible. Fig. 6(c) shows six revolutions that included the last few rubs.

4. RESULTS AND DISCUSSION

The measurements obtained simultaneously from load cells, accelerometers and strain gauges [when the rub blade is instrumented] during several seconds of data acquisition time offer a detailed description of the rub phenomena. Still photography executed after each experiment is also very useful to document casing and blade conditions following several rub strikes. The ability to obtain high-speed imaging of the blade deformations during, between, and immediately after successive casing strikes has been incorporated into the LSPF, and such imaging has been obtained. The purpose of this paper is to describe the facility design and operation and the measurements below for a typical fan blade and are used to illustrate the capabilities of the facility. Load cell and strain gauge measurements are also discussed below. The measurements of acceleration are qualitatively very similar to those obtained from the load cells.

A typical history of the fan blade rotor speed decrease during the rub event, the commanded casing motion and the indication of blade contacts are shown from top to bottom in Figure 7.

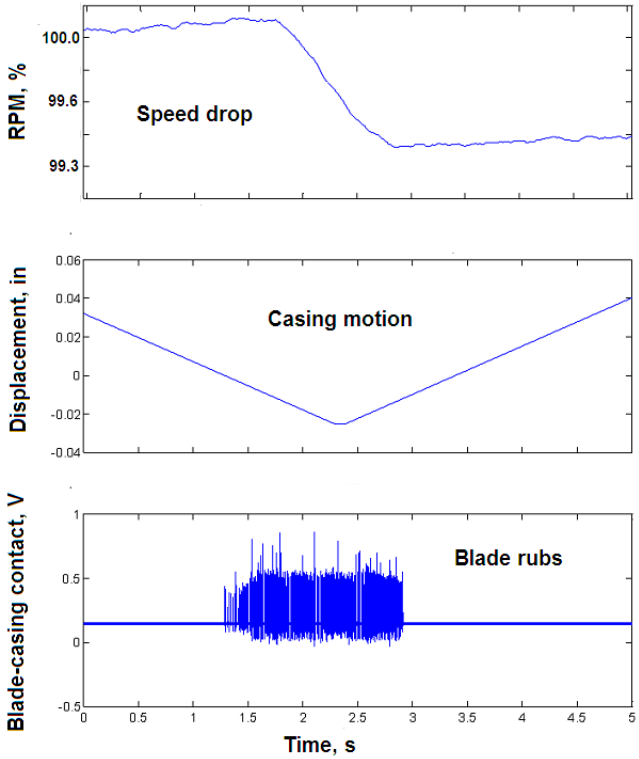

Fig. 7 Typical measurements of (a) Speed Drop, (b) Casing Motion, and (c) Rubs

The measurements are shown for a time period of 5 seconds. At time = 0 the rotor speed is being held nearly constant at just above 100% test-point rpm (Fig.7-a) and the casing is moving toward the spinning blade at the commanded rate of 0.025 in/s (Fig.7-b). Fig. 7 (c) shows all the contacts between the blade and the casing which were shown individually earlier in Fig. 6. Approximately at time = 1.29 s the casing touches the spinning blade, the casing then continues to move inward increasing progressively the interference to a maximum depth of 635 µm (0.025 in), which is reached after 1 additional second of travel at time = 2.3 s. Starting at about 1.8 s the rubs are sufficiently intense that the rotor begins to decelerate even as a constant torque is maintained by supplying unchanged pressure to the driving air turbine. The rate of speed drop was measured at 41.9 rpm/s. After reaching the maximum interference position, the casing dwells for 0.1 s then retracts at a rate of 635 µm/s (0.025 in/s). The record of Fig.7-c shows that contacts between the blade tip and the casing continue to occur until 2.9 s have elapsed. Shortly before that time the rotor stops decelerating, having dropped 40 rpm, and begins to slowly increase speed.

A few photographic records from the experiments with a single blade on the disk impacting on the 90 degrees casing sector coated with abradable are shown in Figures 8 to 10. The simple technique of spraying a light coating of conductive paint on the abradable surface before each experiment was sufficient to successfully visualize the location and extent of blade tip contact to the engine casing sector. The method is readily implemented and effective to visualize even grazing rubs. The use of the conductive paint also ensures that successive blade strikes are recorded as illustrated in Figure 7-c. The obvious drawback of post-experiment photography is that is presents an integrated record of multiple strikes.

Figure 8 shows the casing after two very light rubs. Pretest predictions indicated that the combined axial, radial and circumferential deformation of the airfoil would result in the tip surface coming into contact with the contoured casing surface at the leading edge of the airfoil. The prediction was verified by the experiment. The angular length of the rubs was measured at 22 degrees and 43 degrees. Only a fraction of the chord has developed in both cases [4% and 18%]. Comparing the mark left by the leading edge of the blade tip to the reference line marked on the abradable surface before spinning the rotor indicates the forward axial displacement of the airfoil.

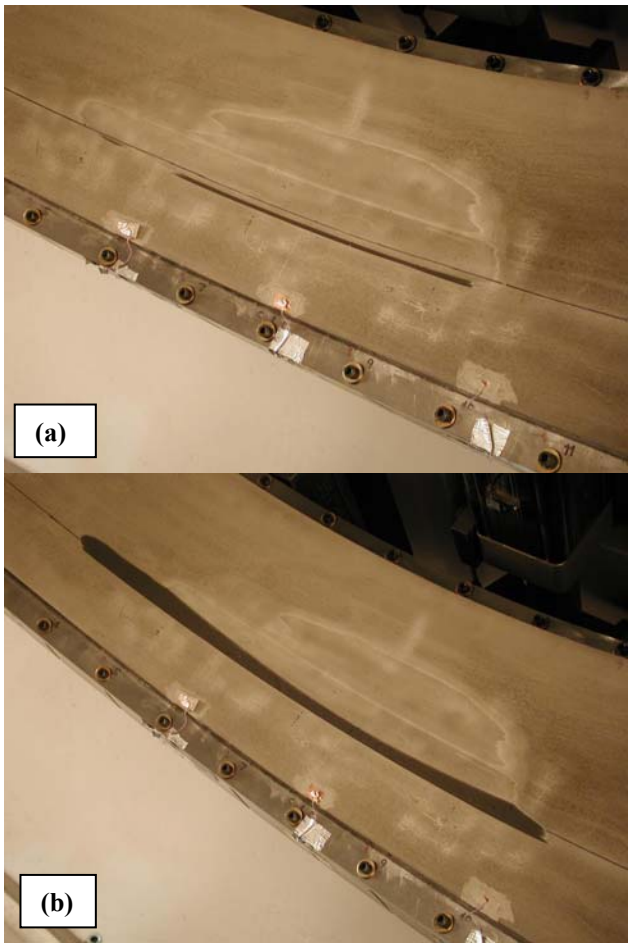

Figure 8 The abradable after two very light rubs. (a) incursion rate 0.010 in/s to a depth of 0.010 in; (b) incursion rate 0.010 in/s to a depth of 0.020 in.

Figure 9 shows the casing after one experiment resulting in a moderate rub with a substantial arc extent [77 degrees] but still a partial chord extent [43%].

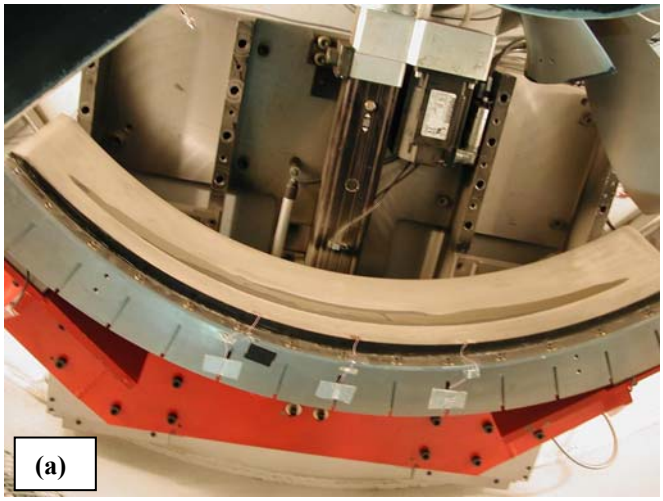

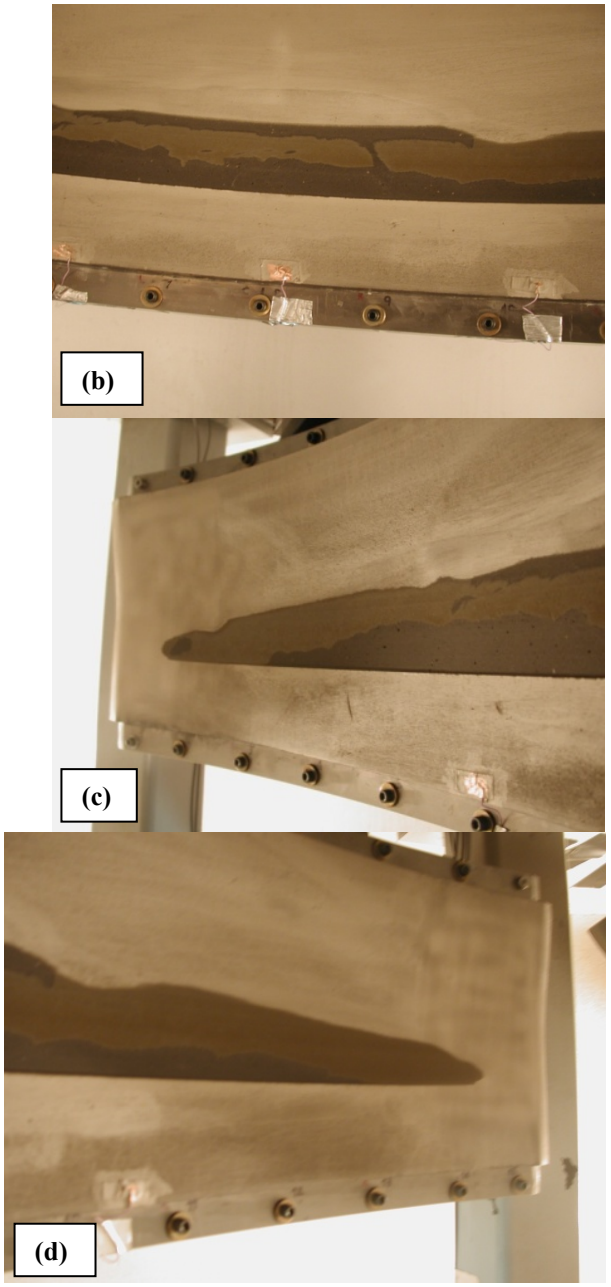

Fig. 9 Casing abradable after one moderate rub. (a) incursion rate 0.025 in/s to a depth of 0.025 in; (b) Close up at the center of the rub area; (c) close up at the entrance of the rub area; (d) close up at the exit of the rub area .

Figure 10 shows the casing after one experiment resulting in a full chord rub. Again there is a substantial arc extent [~85 degrees]. The rotor speed drop was on the order of 100 rpm at a rate of about 74 rpm/s during the experiment.

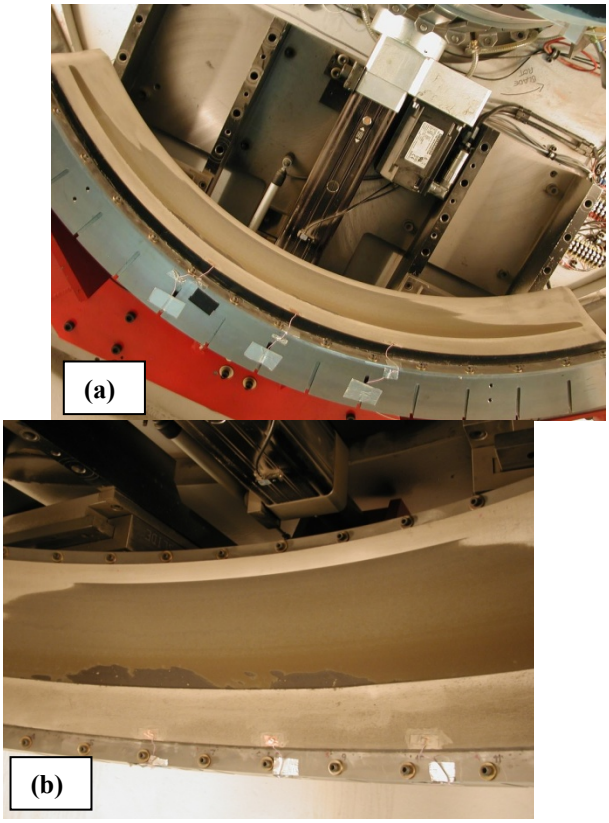

Fig. 10 Casing abradable after a full-chord rub. (a) incursion rate 0.020 in/s to a depth of 0.030 in; (b) Close up at the center of the rub area.

Figure 11 shows a close-up of the tip of the blade at the end of the rub experiments. Under the rub conditions accumulated on this blade there were no signs of plastic deformation or significant burrs at the tip. The browning of metal surface is the only indication of the severity of the conditions encountered by the blade.

Fig. 11 Close-up of the tip of the blade after several rub experiments.

The three load cell measurements from top to bottom of Figure 12 are for the first cell, center cell, and last cell passed by the blade during each revolution. Each cell measures initially small pre-rub inertial loads due to vibrations of the LMU while the rotor is spinning. The magnitude of the pre-rub loads is dependent on cell location. Then the rub loads occur over a time interval of 1.1 s and are readily identified in the figure. Finally, note how quickly after the rub interval the measured loads return to the pre-rub level.

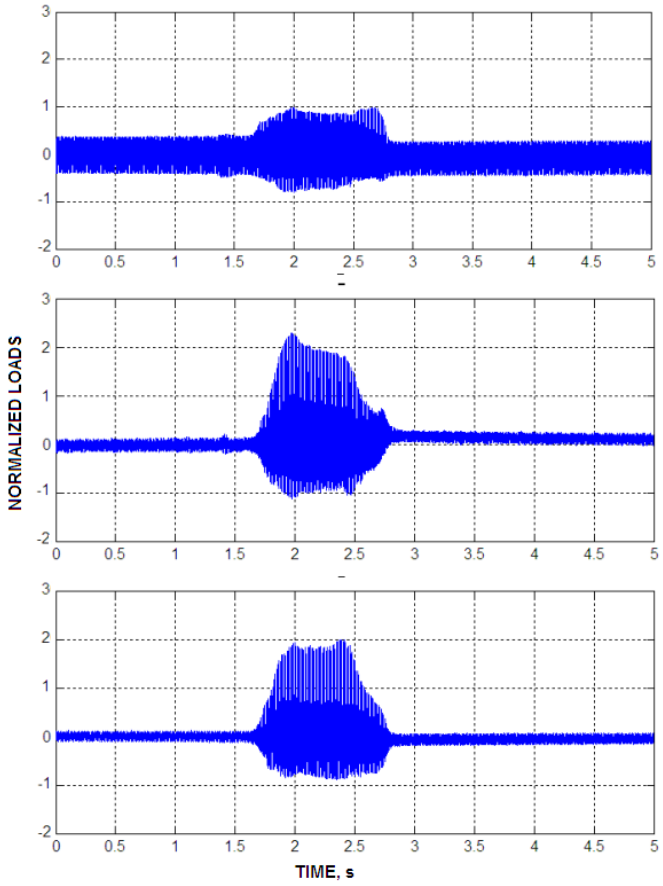

Figure 12 Typical Load Cell Measurements

As the blade rubs on the engine-case segment attached to the LMU, blade tip loads are distributed to the three LMU load cells via the rigid transfer bar. Thus the LMU acts as a mechanical filter on the tip loads. A transfer Frequency Response Function (FRF) algorithm is needed in relating engine-casing loads to load cell measurements. In brief, the theory for the FRF algorithm is based on characterizing the LMU dynamics by impulse vibration testing, whereby the output response at location $\mathbf{x}_0$ is given by:

$$u(x_0, t) = H_{oi}(\omega) F_i e^{j\omega t}$$

Where $\mathbf{H_{oi}(\omega)}$ is the output FRF at location **o** per unit force applied at location **i**.

In order to implement the FRF algorithm to measurements from any of the LMUs used in the spin-pit facilities, the procedure is as follows. Prior to conducting rub experiments, input loads from an impulse hammer are applied at three locations, and in three directions for each location. At the same time, nine response measurements are recorded from the load cells. The elements of the matrix $\mathbf{H_{oi}(\omega)}$ are computed as ratios of measured outputs to known inputs in the frequency domain. Then the inverse of the output FRF matrix is computed and stored for later use in conjunction with rub measurements.

During a rub experiment, nine response measurements are recorded from an unknown force at the rub surface. It is precisely this resultant force that is computed from the known instantaneous blade position and from the inverse of the output FRF operating on the load cell measurements transformed to the frequency domain. The computation above is then repeated for a discrete set of blade positions during the rub.

Experience with several LMU setups combined with detailed finite element structural modeling has shown that issues associated with the practical requirements of impulse vibration testing restrict the application of the FRF algorithm. First order results were obtained for two components of the blade tip load, the radial and the circumferential component. However, refinements in the combined computational and experimental modal characterization are still needed to obtain a precise and validated design method. In the mean time, even with the current method restriction, interesting comparisons of tip loads have been obtained and have been applied to guide the search for stable and reduced-load tip rubs.

For the rub experiments described here, the fan airfoil was not instrumented with strain gauges. However the LSPF has been run in additional measurement programs were measurements of strain and temperature on the blade have been obtained.

5. CONCLUSIONS

A large in-ground spin-pit facility specifically designed to investigate aeromechanic phenomena for gas turbine engine hardware rotating at engine speed is operational at the OSU Gas Turbine Laboratory. The facility extends the capability of a smaller facility in operation since 2002 at GTL. Soon after the commissioning checkouts, the facility was applied to perform blade-casing tip-rub experiments using an engine fan disk with a Ti-alloy airfoil and the associated engine casing coated by abradable. The experiments were designed to obtain specific information related to prediction and modeling of blade-casing interactions.

The results presented in this paper show that progressive incursions of varying severity can be obtained with a high degree of precise control. Several rubs are repeated under various incursion rates for investigation of tip loads and rub arc length progression. In the future, refinements in tip load measurements will be obtained from finite elements modeling and the effect on rub forces and blade dynamics from varying incursion rate will be investigated.

The purpose of this paper was confined to describing the facility design and operation and experimental results were presented to demonstrate the operability of the facility. It is interesting to note that a blade is capable of sustaining incursions that are significant without adverse effects. The dynamics of high-frequency disturbances occurring at blade first contact and at detachment can be characterized relative to low-frequency oscillations in repeated rubs. An indication of tip loads is also available.

In combination with refined design methods and refined modeling of frictional forces, the greater understanding of the phenomena that affect blade-casing interactions is expected to result in savings in gas turbine maintenance costs applicable not only in propulsion engines but for stationary advanced power systems as well.

ACKNOWLEDGMENTS

The work described in this paper was performed as part of the General Electric University Strategic Alliance program at The Ohio State University. Several GE engineers are contributing valuable research directions and assistance to the tip rub project. The authors wish to especially acknowledge the contributions of Jim Rhoda, Steve Manwaring, A.J. Wang, Sunil Sinha, Alan Turner, Dave Pugh, Darin DiTommaso and Jeremy Ferguson. We also would like to acknowledge the contributions to foundation work on tip-rubs by Professor Maurice Adams of Case Western Reserve University.

Several engineers, technicians and students at GTL have supported the experimental and analytical work during past years. Without their skills, initiative and dedication the reported results would have not been possible. Among the many, the authors wish to mention on this occasion Charlie Haldeman, John Newkirk, Ken Copley, Ken Fout, Michael Wehri, Kelsey Edwards, and Matt Smith.

REFERENCES

[1] Padova, C., Barton, J., Dunn, M.G., Manwaring, S., Young, G., Adams, M.L., and Adams, M., 2005. “Development of an Experimental Capability to Produce Controlled Blade Tip / Shroud Rubs at Engine Speed,” Journal of Turbomachinery, Vol. 127, pp. 726-735

[2] Padova, C., Barton, J., Dunn, M.G., Manwaring, S., 2007. “Experimental Results from Controlled Blade Tip / Shroud Rubs at Engine Speed,” Journal of Turbomachinery, Vol. 129, pp. 713-723.

[3] Padova, C., Dunn, M.G., Barton, J., Turner, K., Turner, A., DiTommaso, D., 2010. “Casing Treatment and Blade-Tip Configuration Effects on Controlled Gas Turbine Blade Tip/Shroud Rubs at Engine Conditions,” Journal of Turbomachinery, Vol.133, 011016-pp 1-12.

[4] Kosing, O.E., Scharl, R., and Schmuhl, H.J., 2001 "Design Improvements of the EJ 200 HP Compressor. From Design Verification Engine to a Future All Blisk Version," ASME 2001-GT-0283

[5] Greitzer, E.M., Nikkanen J.P., Haddad D.E., Mazzaway R.S., and Joslyn H.D., 1979. "A Fundamental Criterion for the Application of Rotor Casing Treatment," ASME J. Fluids Eng., Vol.101, pp 237-243.

[6] Voges M., Schnell R., Willert C., Mönig R., Müller M.W., and Zscherp C., 2011. "Investigation of Blade Tip Interaction with Casing Treatment in a Transonic Compressor," Journal of Turbomachinery, Vol.133, 011007-pp 1-11.

[7] Storace, A.F., Wisler, D.C., Shin, H.W., Beacher, B.F., Ehrich, F.F., Spakovszky, Z.S., Martinez-Sanchez, M., and Song, S.J., 2001 "Unsteady Flow and Whirl-Inducing Forces in Axial-Flow Compressors: Part I – Experiment," J. Turbomachinery, Vol. 123, pp 433-445

[8] Ehrich, F.F., Spakovszky, Z.S., Martinez-Sanchez, M., Song, S.J., Wisler, D.C., Storace, A.F., Shin, H.W., Beacher, B.F., 2001 "Unsteady Flow and Whirl-Inducing Forces in Axial-Flow Compressors: Part II – Analysis," J. Turbomachinery, Vol. 123, pp 446-453

[9] Turner, K., Adams, M.L., and Dunn, M.G., 2005. "Simulation of Engine Blade Tip-Rub Induced Vibration," GT2005-68217, Proceedings of ASME Turbo Expo 2005Power for Land, Sea, and Air June 6–9, Reno-Tahoe, Nevada USA.

[10] Sinha, S.K., 2007. "Combined Torsional-Bending-Axial Dynamics of a Twisted Rotating Cantilever Timoshenko Beam with Contact-Impact Loads at the Free End," Journal of Applied Mechanics, Vol. 74, pp. 505-522.

[11] Turner, K., Dunn, M.G., Padova, C., 2010. "Airfoil Deflection Characteristics During Rub Events," GT2010-22166, Proceedings of ASME Turbo Expo 2010: Power for Land, Sea, and Air June 14–18, Glasgow, UK.

[12] Ferguson, J., Dunn, M.G., Padova, C., Manwaring, S., Turner, A., 2010. "A Moving Load Finite Element-Based Approach to Determination of Case Load in a Blade-on-Casing Incursion," GT2010-22048, Proceedings of ASME Turbo Expo 2010: Power for Land, Sea, and Air June 14–18, Glasgow, UK.

[13] Muszynska, A., 1989. "Rotor-to-Stationary Element Rub-Related Vibration Phenomena in Rotating Machinery – Literature Survey," Shock and Vibration Digest, Vol. 21, pp. 3-11.

[14] Padovan, J., and Choy F.K., 1987. "Nonlinear Dynamics of Rotor/Blade/Casing Interactions," Journal of Turbomachinery, Vol. 109, pp. 527-534.

[15] Adams, M.L., 2000. Rotating Machinery Vibration. From Analysis to Troubleshooting. Marcel Dekker Inc., N.Y.

[16] Manwaring, S.R., and Wisler, D.C., 1993. "Unsteady Aerodynamics and Gust Response in Compressors and Turbines," Journal of Turbomachinery, Vol. 115.

[17] Kielb, J.J., Abhari, R.S., and Dunn, M.G., 2001. "Experimental and Numerical Study of Forced Response in a Full-Scale Rotating Turbine," ASME 2001-GT-0263

[18] Laverty, W.F., 1981. "Rub Energetics of Compressor Blade Tip Seals," Proceedings of the 3th International Conference on Wear of Materials, pp. 714-721.

[19] Liu, S., and Wang, Q.J., 2007. "Determination of Young's Modulus and Poisson's Ratio for Coatings," Surface & Coatings Technology 201, pp. 6470-6477.